Electronic Supplementary Material (ESI) for Dalton Transactions.

Supramolecular frameworks based on 5,10,15,20-tetra(4-carboxyphenyl)porphyrins

Mahbod Morshedi,[a] Jas S. Ward,[a,b] Paul E. Kruger[b] and Nicholas G. White[a]*

[a]*Research School of Chemistry, Australian National University*

137 Sullivan's Creek Road, Acton, 2601, ACT, Australia

Email: nicholas.white@anu.edu.au

URL: www.nwhitegroup.com

[b]*MacDiarmid Institute for Advanced Materials and Nanotechnology, School of Physical and Chemical Sciences, University of Canterbury, Christchurch 8140, New Zealand*

Experimental considerations and details of instrumentation

1·4Cl,[S1] **2·2Cl**,[S2] **3·2Cl**,[S2] **4^{4H}** [S3], and **5^{4H}** [S3] were prepared as previously described. Other chemicals were bought from commercial suppliers and used as received.

NMR spectra were collected on Varian Gemini, Bruker Avance 400 or Bruker Avance 700 spectrometers and are referenced to the residual solvent signal.[S4] Infrared spectra were recorded on a Perkin-Elmer Spectrum Two FT-IR Spectrometer fitted with an ATR Two Single Reflection Diamond. PXRD data were recorded at room temperature on a PANalytical Empyrean diffractometer using Cu Kα radiation and a PIXcel detector. Elemental analyses were recorded at London Metropolitan University.

Electrospray ionisation mass spectrometry data were acquired on a Micromass Waters ZMD spectrometer. All compounds apart from [**4^{4H}**·(**bpy**)$_2$·(DMSO)$_2$]$_n$ were insoluble in all tested solvents, and so it was necessary to digest the samples using $HCl_{(aq)}$ before obtaining mass spectrometry data (from methanol). [**4^{4H}**·(**bpy**)$_2$·(DMSO)$_2$]$_n$ is soluble in DMSO/methanol, so this acid digestion step was not necessary.

Additional characterisation for $[1{\cdot}4]_n$ and $[4^{4H}{\cdot}(bpy)_2{\cdot}(DMSO)_2]_n$

^{1}H NMR spectrum of $[1{\cdot}4]_n$:

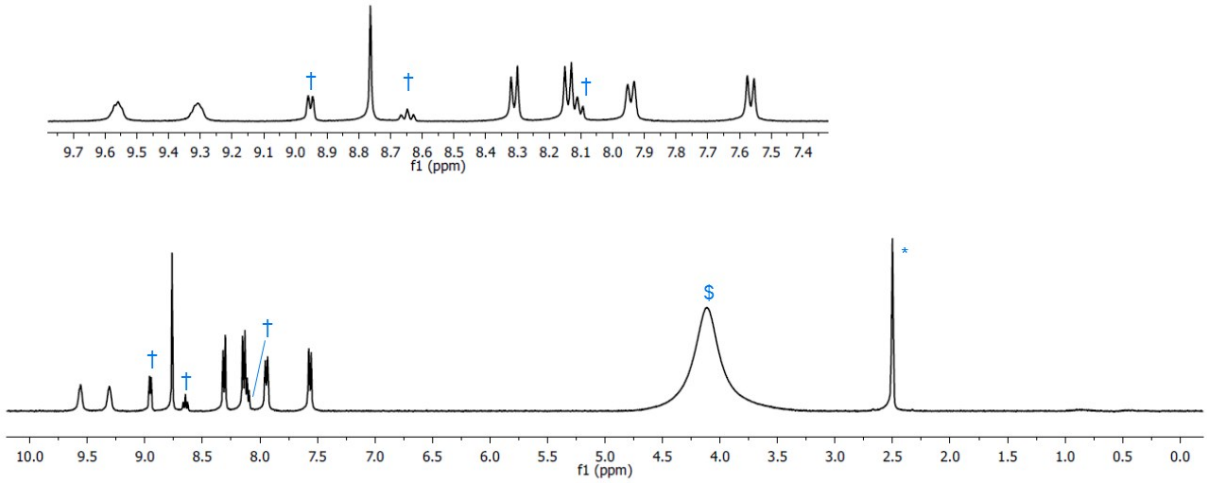

Figure S1. ^{1}H NMR spectrum of $[\mathbf{1}{\cdot}\mathbf{4}]_n$ (400 MHz, 298 K, d_6-DMSO containing a drop of $DCl_{(aq)}$, peak marked * corresponds to residual solvent signal, peak marked $ corresponds to water, peaks marked † correspond to residual pyridine that is not removed even after drying).

PXRD pattern of $[1{\cdot}4]_n$:

As can be seen from Figure S2, $[\mathbf{1}{\cdot}\mathbf{4}]_n$ rapidly loses crystallinity when removed from solvent.

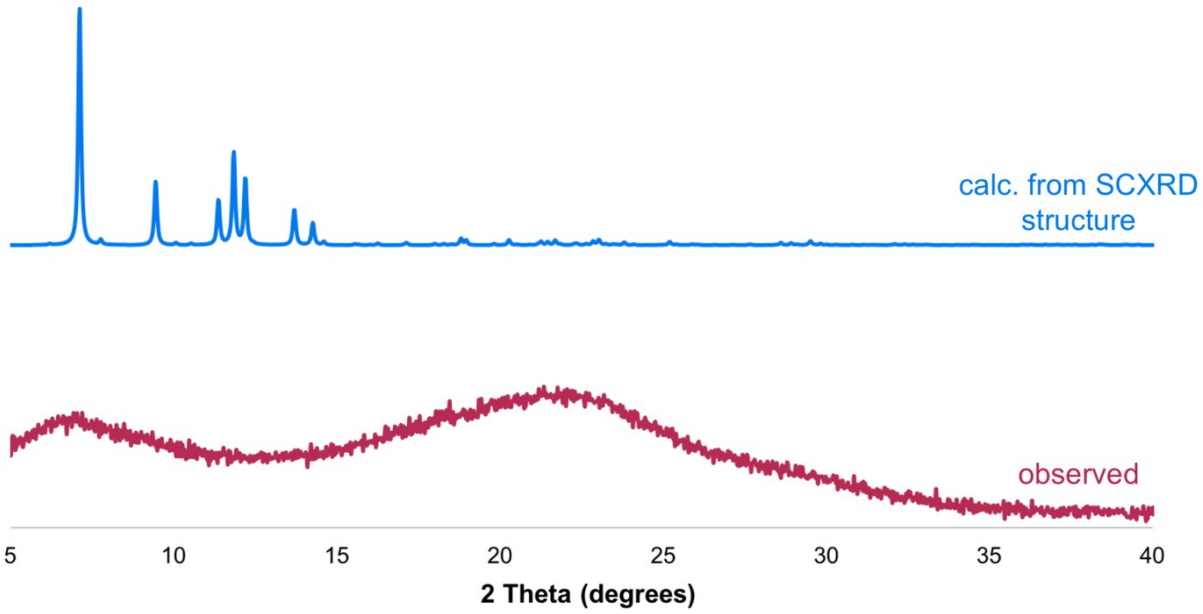

Figure S2. PXRD pattern of $[\mathbf{1}{\cdot}\mathbf{4}]_n$.

[4^{4H}·(bpy)$_2$·(DMSO)$_2$]$_n$:

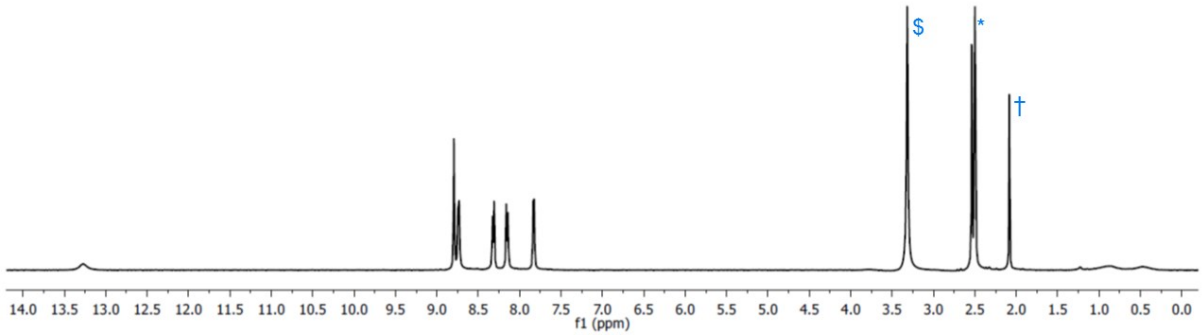

Figure S3. ^{1}H NMR spectrum of [**4**^{4H}·(**bpy**)$_2$·(DMSO)$_2$]$_n$ (400 MHz, 298 K, d_6-DMSO; peak marked * corresponds to residual solvent signal, peak marked $ corresponds to water, peak marked † corresponds to residual acetone).

PXRD pattern of [4^{4H}·(bpy)$_2$(DMSO)$_2$]$_n$:

The measured PXRD pattern of [**4**^{4H}·(**bpy**)$_2$(DMSO)$_2$]$_n$ (Figure S4, recorded at 293 K) is approximately consistent with that calculated from the SCXRD structure (recorded at 150 K) suggesting that the structure determined by SCXRD is consistent with the bulk material.

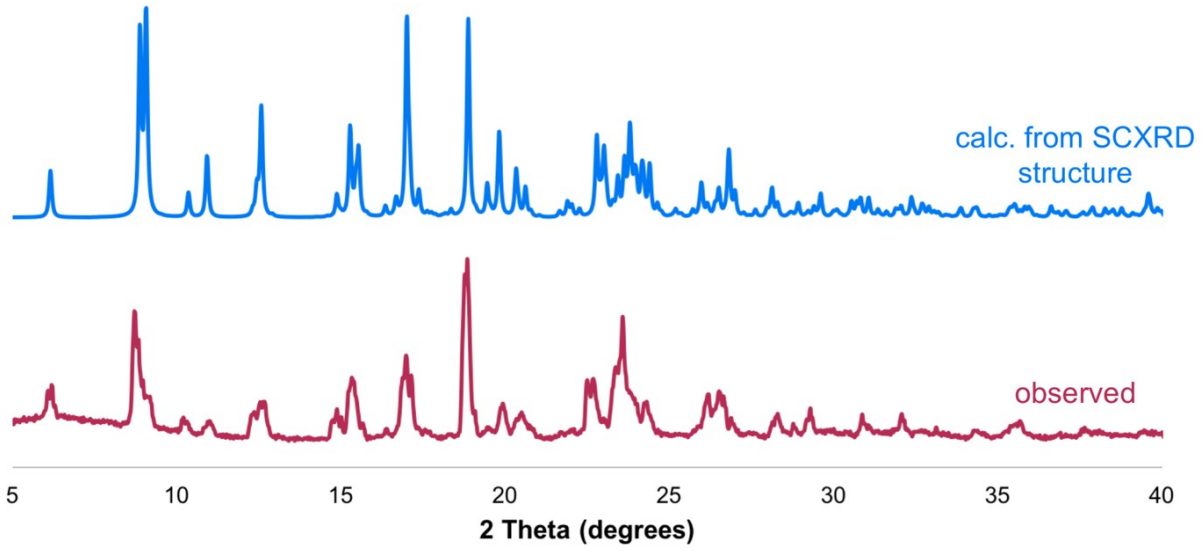

Figure S4. PXRD pattern of [**4**^{4H}·(**bpy**)$_2$·(DMSO)$_2$]$_n$.

^{1}H NMR spectrum of 4^{4H} upon addition of pyridine

The ^{1}H NMR spectrum of $\mathbf{4^{4H}}$ is sharp suggesting a diamagnetic (*i.e.* square planar) nickel(II) centre, with minimal coordination of DMSO in the axial positions. Addition of four equivalents of pyridine results in only minimal shifts in the porphyrin pyrrole protons, suggesting negligible interaction with the nickel(II) ion. In related systems, an apically-coordinating pyridyl donor results in shifts of > 30 ppm.[S5] No shift is observed in the position of the carboxylic acid resonance, suggesting minimal hydrogen bonding interactions in the competitive solvent used.

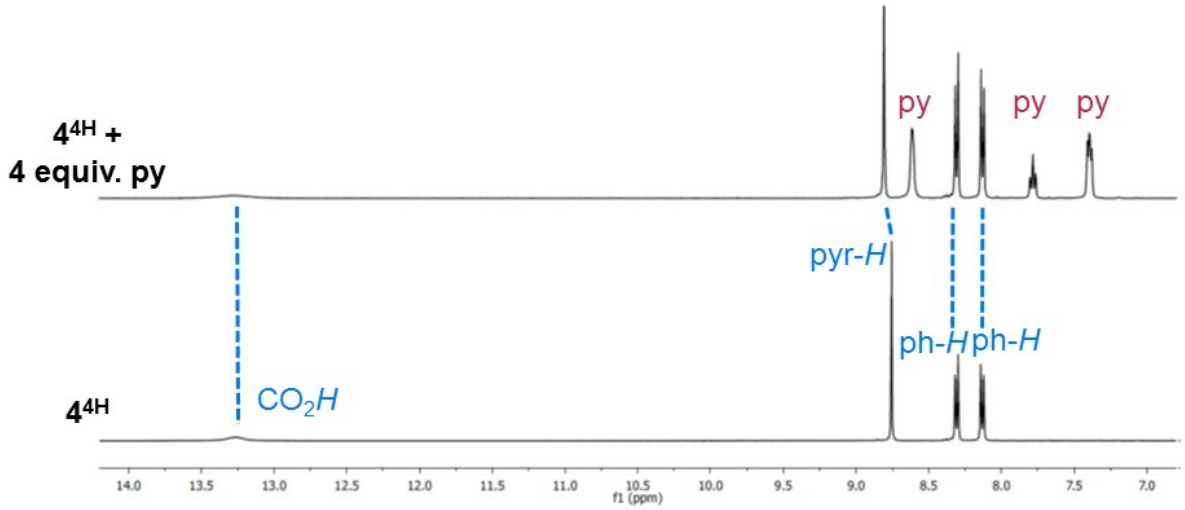

Figure S5. ^{1}H NMR spectrum of $\mathbf{4^{4H}}$ before and after addition of four equivalents of pyridine (400 MHz, 298 K, d_6-DMSO).

Synthesis and characterisation of other compounds

1·5

A solution of **1·4Cl** (16 mg, 0.025 mmol) in water (2 mL) was carefully layered with pyridine (1 mL) and then a solution of $\mathbf{5}^{\mathbf{4H}}$ (20 mg, 0.025 mmol) in pyridine (2 mL). After 5 days, the resulting purple crystals were isolated by filtration, washed with water (3 × 2 mL) and air-dried to give 1·**5** as dark purple crystals. Yield: 20 mg (0.016 mmol, 62%).

^{1}H NMR [d_6-DMSO containing 1 drop $DCl_{(aq)}$]: 9.58 (br. s, 8H), 9.32 (br. s, 8H), 8.82 (br. s, 8H), 8.70 (s, 8H), 8.65 (d, *J* = 7.6 Hz, 8H), 7.95 (d, *J* = 7.8 Hz, 8H), 7.56 (d, *J* = 7.8 Hz, 8H). ESI-MS (pos.): 791.4, calc. for $C_{48}H_{31}N_4O_8^+$, *i.e.* [$\mathbf{5}^{\mathbf{4H}}$·H]$^+$: 791.2; 245.3, calc. for $C_{29}H_{30}N_8^{2+}$, *i.e.* [**1** –2H]$^{2+}$: 245.1 Da. IR (ATR, *inter alia*): 1669, 1580, 1532, 1480, 1373 cm^{-1}.

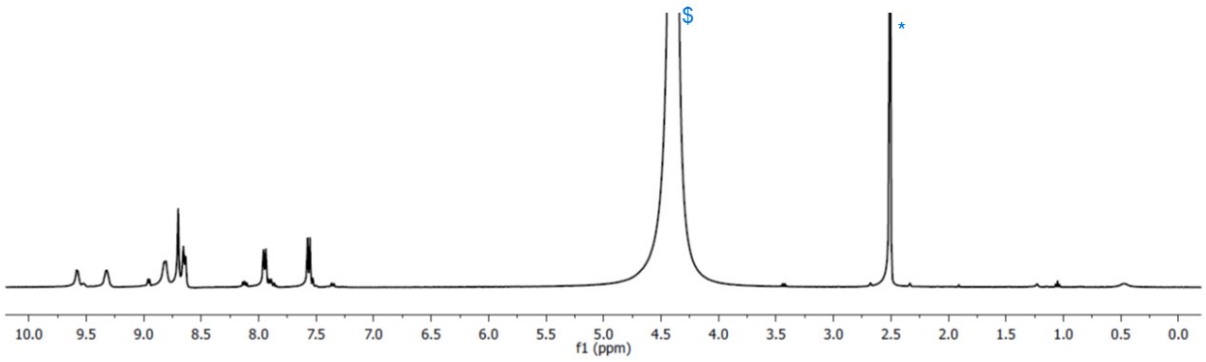

Figure S6. ^{1}H NMR spectrum of **1·5** (400 MHz, 298 K, d_6-DMSO containing a drop of $DCl_{(aq)}$, peak marked * corresponds to residual solvent signal, peak marked $ corresponds to water).

2_2·4

A solution of **2·2Cl** (9.4 mg, 0.040 mmol) in water (2 mL) was carefully layered with pyridine (1 mL), then a solution of $\mathbf{4}^{\mathbf{4H}}$ (16 mg, 0.020 mmol) in pyridine (2 mL). After 5 days, the resulting purple crystals were isolated by filtration, washed with water (3 × 2 mL) and air-dried to give $\mathbf{2_2}$·**5**. Yield: 13 mg (0.012 mmol, 56%).

^{1}H NMR [d_6-DMSO containing 1 drop $DCl_{(aq)}$]: 9.75 (br. s, 8H), 9.50 (br. s, 8H), 8.76 (s, 8H), 8.30 (d, *J* = 8.0 Hz, 8H), 8.13 (d, *J* = 8.0 Hz, 8H), 8.05 (s, 8H). ESI-MS (pos.): 163.1, calc. for $C_8H_{11}N_4^+$, *i.e.* [**3**–H]$^+$: 163.1 Da. IR (ATR, *inter alia*): 1664, 1581, 1534, 1475, 1378 cm^{-1}.

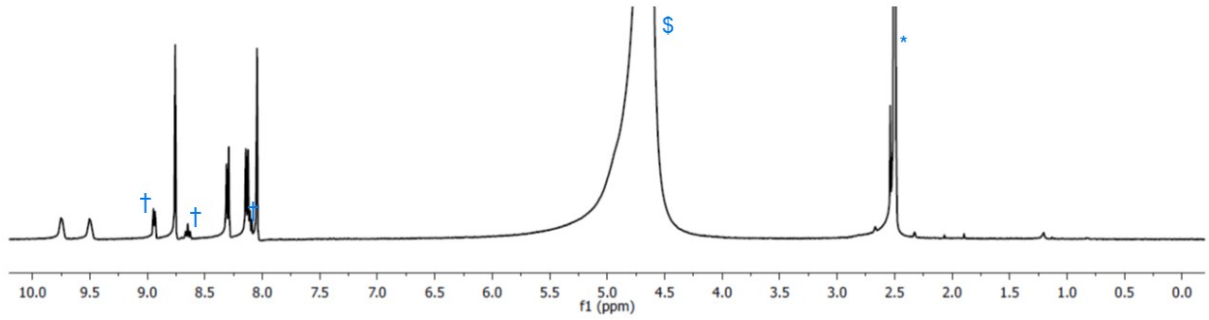

Figure S7. ^{1}H NMR spectrum of $\mathbf{2_2}$·**4** (400 MHz, 298 K, d_6-DMSO containing a drop of $DCl_{(aq)}$, peak marked * corresponds to residual solvent signal, peak marked $ corresponds to water, peaks marked † correspond to residual pyridine).

2_2·5

A solution of **2·2Cl** (9.4 mg, 0.040 mmol) in water (2 mL) was carefully layered with pyridine (1 mL), then a solution of **5^{4H}** (16 mg, 0.020 mmol) in pyridine (2 mL). After 5 days, the resulting purple crystals were isolated by filtration, washed with water (3 × 2 mL) and air-dried to give **2_2·5**. Yield: 13 mg (0.012 mmol, 58%).

^{1}H NMR [d_6-DMSO containing 1 drop $DCl_{(aq)}$]: 9.76 (br. s, 8H), 9.49 (br. s, 8H), 8.81 (d, *J* = 8.0 Hz, 8H), 8.68 (s, 8H), 8.64(d, *J* = 8.0 Hz, 8H), 8.05 (s, 8H). ESI-MS (pos.): 791.4, calc. for $C_{48}H_{31}N_4O_8^+$, *i.e.* [**5^{4H}**·H]$^+$: 791.2; 163.0, calc. for $C_8H_{11}N_4^+$, *i.e.* [**3**–H]$^+$: 163.1 Da. IR (ATR, *inter alia*): 1584, 1537, 1476, 1441, 1383, 1350 cm^{-1}.

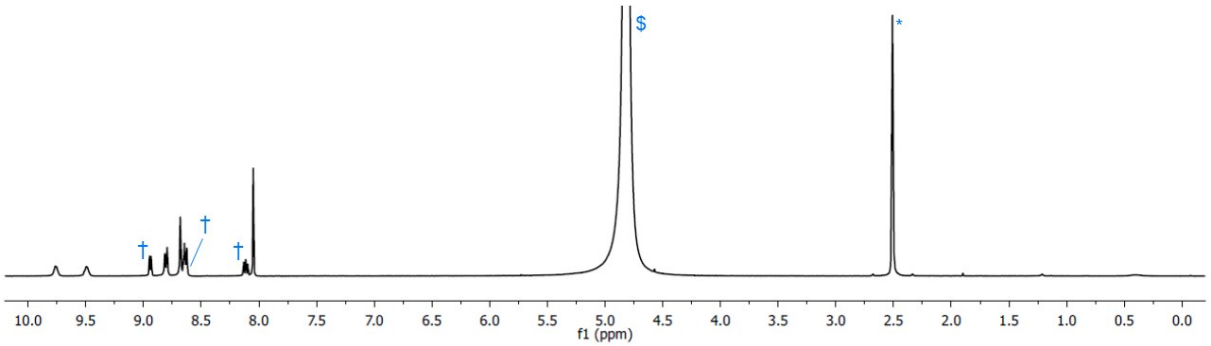

Figure S8. ^{1}H NMR spectrum of **2_2·5** (400 MHz, 298 K, d_6-DMSO containing a drop of $DCl_{(aq)}$, peak marked * corresponds to residual solvent signal, peak marked $ corresponds to water, peaks marked † correspond to residual pyridine).

3_2·4

A solution of **4^{4H}** (17 mg, 0.020 mmol) in pyridine (2 mL) was added to a solution of **3·2Cl** (9.4 mg, 0.040 mmol) in water (3 mL). The resulting purple solution was subjected to acetone vapour diffusion, resulting in the formation of purple crystals. These were isolated by filtration, washed with water (3 × 2 mL) and air-dried to give **3_2·4**. Yield: 21 mg (0.018 mmol, 90%).

^{1}H NMR [d_6-DMSO containing 1 drop $DCl_{(aq]}$: 9.76 (br. s, 8H), 9.48 (br. s, 8H), 8.77 (s, 8H), 8.50 (s, 2H), 8.31 (d, *J* = 8.1 Hz, 8H), 8.13–8.17 (m, 12H), 7.83 (t, *J* = 7.8 Hz, 2H) ppm. ESI-MS (pos.): 163.2, calc. for $C_8H_{11}N_4^+$, *i.e.* [**3**–H]$^+$: 163.1 Da. IR (ATR, *inter alia*): 1673, 1581, 1520, 1371, 1349 cm^{-1}.

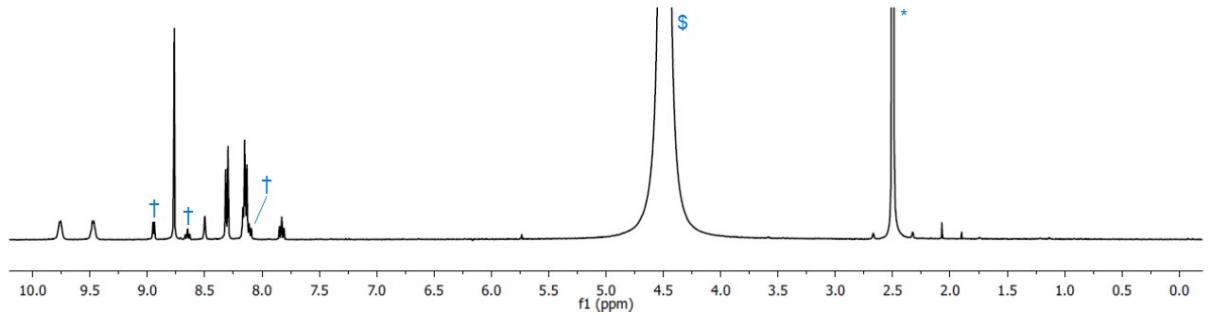

Figure S9. ^{1}H NMR spectrum of **3_2·4** (400 MHz, 298 K, d_6-DMSO containing a drop of $DCl_{(aq)}$, peak marked * corresponds to residual solvent signal, peak marked $ corresponds to water, peaks marked † correspond to residual pyridine).

3_2·5

A solution of **5^{4H}** (20 mg, 0.025 mmol) in pyridine (2 mL) was added to a solution of **3·2Cl** (12 mg, 0.050 mmol) in water (3 mL). The resulting purple solution was subjected to acetone vapour diffusion, resulting in the formation of purple crystals. These were isolated by filtration, washed with water (3 × 2 mL) and air-dried to give **3_2·5**. Yield: 18 mg (0.016 mmol, 64%).

^{1}H NMR [d_6-DMSO containing 1 drop $DCl_{(aq)}$: 9.75 (br. s, 8H), 9.46 (br. s, 8H), 8.80 (br. s, 8H), 8.70 (s, 8H), 8.64 (d, *J* = 7.6 Hz, 8H), 8.49 (s, 2H), 8.16 (d, *J* = 7.8 Hz, 4H), 7.83 (t, *J* = 7.8 Hz, 2H) ppm. ESI-MS (pos.): 791.4, calc. for $C_{48}H_{31}N_4O_8^+$, *i.e.* [**5^{4H}**·H]$^+$: 791.2; 163.0, calc. for $C_8H_{11}N_4^+$, *i.e.* [**3**–H]$^+$: 163.1 Da. IR (ATR, *inter alia*): 1679, 1579, 1522, 1470, 1378 cm^{-1}.

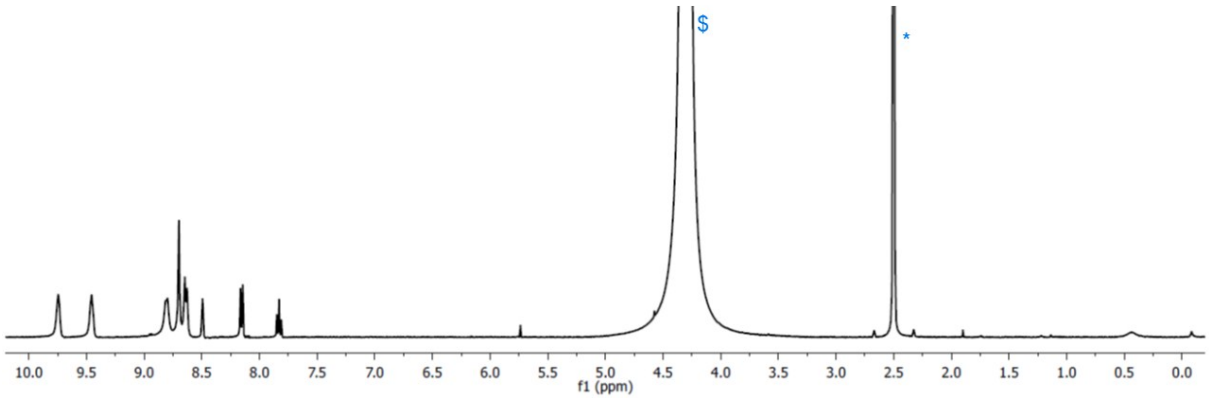

Figure S10. ^{1}H NMR spectrum of **3_2·5** (400 MHz, 298 K, d_6-DMSO containing a drop of $DCl_{(aq)}$, peak marked * corresponds to residual solvent signal, peak marked $ corresponds to water).

4^{4H}·$(py)_6$

Single crystals of **4**·$(py)_6$ were obtained by diffusing diethyl ether vapour into a solution of **4^{4H}** in pyridine.

5^{4H}·$(py)_4$

Single crystals of **5**·$(py)_4$ were obtained by diffusing diethyl ether vapour into a solution of **5^{4H}** in pyridine.

Single crystal X-ray diffraction (SCXRD)

General comments on SCXRD

*Structure of [**1**·**4**]$_n$:*

Data for this structure were collected at the Australian Synchrotron on the MX1 beamline using silicon double crystal monochromated synchrotron radiation at 100 K. Raw frame data were collected using BluIce,[S6] and data reduction, interframe scaling, unit cell refinement and absorption corrections were processed using XDS.[S7]

The structure was solved with ShelXT[S8] and refined using ShelXL[S9] in OLEX2.[S10] All non-hydrogen atoms were refined with anisotropic displacement parameters. C–H hydrogen atoms were placed geometrically and refined with riding restraints on their parent atoms. N–H hydrogen atoms were placed geometrically and their positions refined, but with riding restraints for U_{iso} values.

All other structures:

Data for all structures other than [**1**·**4**]$_n$ were collected using mirror-monochromated Cu Kα radiation on an Agilent SuperNova diffractometer. Crystals were cooled to 150 K using a Cryostream N2 open-flow cooling device[S11] in all cases. Raw frame data (including data reduction, interframe scaling, unit cell refinement and absorption corrections) were processed using CrysAlisPro.[S12]

Structures were solved with SUPERFLIP[S13] and refined using full-matrix least-squares on F^2 within the CRYSTALS suite.[S14] All non-hydrogen atoms were refined with anisotropic displacement parameters. C–H hydrogen atoms were generally visible in the Fourier difference map, and were initially refined with restraints on bond lengths and angles, after which the positions were used as the basis for a riding model.[S15] O–H and N–H hydrogen atoms were generally visible in the Fourier difference map and their positions were refined with restraints on bond lengths and angles.[S15]

Full crystallographic data in CIF format for all structures are provided as Supporting Information (CCDC Numbers: 1574946–1574952 and 1589159). Selected data are summarised in Table S3 and individual structures are discussed in more detail below.

Comments on individual structures

*Structure of [**1**·**4**]$_n$:*

As expected for supramolecular complexes with a high void volume, the data collected for this structure suffered from rapid fall-off of reflection intensity at high diffraction angle, and this had a negative impact on the quality of the high angle reflections, with some not being observed despite the use of synchrotron radiation. PLATON ADDSYM[S16] suggests the presence of the higher symmetry space group *I*4/*mcm*, however it was not possible to solve or refine the structure in this space group. The structure could be refined in the non-centrosymmetric space group *I*4 as an inversion twin [Flack parameter = 0.470(18)].[S17]

Refinement of the structure was complicated by half the molecule being generated over a symmetry operation, which necessitated that FLAT restraints be applied to maintain the planarity of the porphyrin ring. Subsequently, bond lengths (DFIX), bond angles (DANG), thermal and vibrational ellipsoid parameters (RIGU) were restrained for several regions of the model. The only constraint required was for N11, N12 and C13 of the amidinium tetracation, where EADP was used to aid in modelling the thermal ellipsoids of the two nitrogen atoms.

No sensible solvates could be identified and modelled in the substantial void space of the structure, therefore PLATON-SQUEEZE was used to account for the electron density within this part of the cell (75% of the unit cell volume).[S18] While this structure is of low quality, the general connectivity of the framework is readily apparent. As noted in the main text, while it appears that most of the time the nickel(II) ion has a square planar geometry, there is a small amount of residual electron density located close to the ion, which could suggest the presence of axial donors present a small proportion of the time in the crystal (*i.e.* low, partial occupancy donors). Due to the low quality of the data, the identity or occupancy of these could not be determined.

*Structure of **2**$_2$·**5**:*

A region of diffuse electron density was present, believed to arise from disordered solvent molecules. This could not be sensibly modelled and so PLATON-SQUEEZE[S18] was used to include this electron density in the model. Two benzoate groups and one bis-amidinium molecule were poorly behaved, and so it was necessary to add restraints to the bond lengths, and thermal and vibrational ellipsoid parameters of the atoms in these groups to achieve a sensible refinement. Some residual electron density is located about these groups, which could not be modelled.

*Structure of **3**$_2$·**4**:*

A region of diffuse electron density was present, believed to arise from disordered solvent molecules. This could not be sensibly modelled and so PLATON-SQUEEZE[S18] was used to include this electron density in the model. Otherwise no crystallographic restraints were necessary apart from those on O–H and N–H bond lengths and angles.

*Structure of **3**$_2$·**5**:*

A region of diffuse electron density was present, believed to arise from disordered solvent molecules. This could not be sensibly modelled and so PLATON-SQUEEZE[S18] was used to include this electron density in the model. Otherwise no crystallographic restraints were necessary apart from those on O–H and N–H bond lengths and angles.

*Structure of [**4**^{4H}·(**bpy**)$_2$·(DMSO)$_2$]$_n$ crystallised from DMSO/acetone:*

Refinement proceeded smoothly, and no crystallographic restraints were necessary apart from those on O–H bond lengths and angles.

*Structure of [**4**^{4H}·(**bpy**)$_2$·(DMSO)$_2$]$_n$ crystallised from DMSO/dichloromethane:*

Crystals were small and weakly-diffracting, resulting in some high angle reflections not being observed. It was necessary

to apply restraints to the bond lengths, and thermal and vibrational ellipsoid parameters of a dichloromethane solvent molecule in order to achieve a sensible refinement. Some residual electron density is located near to this solvent molecule, which could not be modelled. Otherwise, no crystallographic restraints were necessary apart from those on O–H bond lengths and angles.

*Structure of **4**·(py)$_6$:*

It was necessary to add restraints to the bond lengths, and thermal and vibrational ellipsoid parameters of a diethyl ether solvent molecule to achieve a sensible refinement of this molecule. Otherwise no crystallographic restraints were necessary apart from those on O–H bond lengths and angles.

*Structure of **5**·(py)$_4$:*

Refinement proceeded smoothly, and no crystallographic restraints were necessary apart from those on O–H bond lengths and angles.

Table S3. Selected crystallographic data.

Compound	**$[1\cdot4]_n$[a]**	**$2_2\cdot5$[a]**	**$3_2\cdot4$[a]**	**$3_2\cdot5$[a]**
Formula	$C_4H_4N_4NiO_8$, $C_{29}H_{32}N_8$	1.5($C_{48}H_{26}N_4O_8$), 3($C_8H_{12}N_4$)·*solvents*	$C_{48}H_{24}N_4NiO_8$, 2($C_8H_{12}N_4$), 2(H_2O)·*solvents*	$C_{48}H_{26}N_4O_8$, 2($C_8H_{12}N_4$), 3(C_5H_5N), H_2O·*solvents*
Formula weight	1336.04	1672.76	1207.90	1370.50
a (Å)	17.556(3)	15.6606(3)	10.86990(10)	10.0854(2)
b (Å)	17.556(3)	18.9312(3)	24.1347(2)	20.0861(5)
c (Å)	56.930(11)	20.4250(3)	24.7076(2)	20.4927(5)
α (°)	90	86.1854(13)	90	109.178(2)
β (°)	90	79.7696(15)	90	103.485(2)
γ (°)	90	72.5303(15)	90	103.585(2)
Unit cell volume (Å^3)	17547(6)	5683.78(8)	6481.84(5)	3586.88(9)
Crystal system	tetragonal	triclinic	orthorhombic	triclinic
Space group	*I4*	$P\bar{1}$	*Pnna*	$P\bar{1}$
Z	4	2	4	2
Reflections (all)	42023	118047	104624	118047
Reflections (unique)	11736	22953	6567	13058
R_{int}	0.058	0.043	0.043	0.029
R_1 [$I > 2\sigma(I)$]	0.039	0.080	0.072	0.054
$wR_2(F^2)$ (all data)	0.111	0.225	0.210	0.120

Compound	**$[4^{4H}\cdot(bpy)_2\cdot(DMSO)_2]_n$ ·(*acetone*)$_2$**	**$4^{4H}\cdot(bpy)_2\cdot(DMSO)_2]_n$ ·(*dichloromethane*)$_2$**	**$4\cdot(py)_6$**	**$5\cdot(py)_4$**
Formula	$C_{34}H_{22}N_4Ni_{0.5}O_4$, C_2H_6OS, C_3H_6O	$C_{34}H_{22}N_4Ni_{0.5}O_4$, C_2H_6OS, CH_2Cl_2	0.5($C_{58}H_{38}N_6NiO_8$), ·2(C_5H_5N),·$C_4H_{10}O$	0.5($C_4H_8H_{28}N_4NiO_8$), 2(C_5H_5N), $C_4H_{10}O$
Formula weight	716.15	743.00	735.17	627.72
a (Å)	11.47610(10)	11.4326(6)	12.44400(10)	14.7549(5)
b (Å)	28.7617(2)	29.0833(11)	13.02970(10)	7.3113(3)
c (Å)	11.75310(10)	11.5789(7)	23.3004(2)	30.7507(12)
α (°)	90	90	90	90
β (°)	115.3098(10)	116.102(7)	97.7760(9)	92.163(4)
γ (°)	90	90	90	90
Unit cell volume (Å^3)	3506.99(3)	3457.3(2)	3743.22(3)	3314.95(13)
Crystal system	monoclinic	monoclinic	monoclinic	monoclinic
Space group	$P2_1/n$	$P2_1/n$	$P2_1/c$	$P2_1/c$
Z	4	4	4	4
Reflections (all)	56693	18635	27340	17673
Reflections (unique)	7096	6003	7555	5994
R_{int}	0.031	0.043	0.022	0.060
R_1 [$I > 2\sigma(I)$]	0.041	0.083	0.039	0.059
$wR_2(F^2)$ (all data)	0.101	0.185	0.104	0.143

[a] PLATON-SQUEEZE[S18] used.

Structure of $[4^{4H}\cdot(bpy)_2\cdot(DMSO)_2]_n$ crystallised from DMSO/DCM

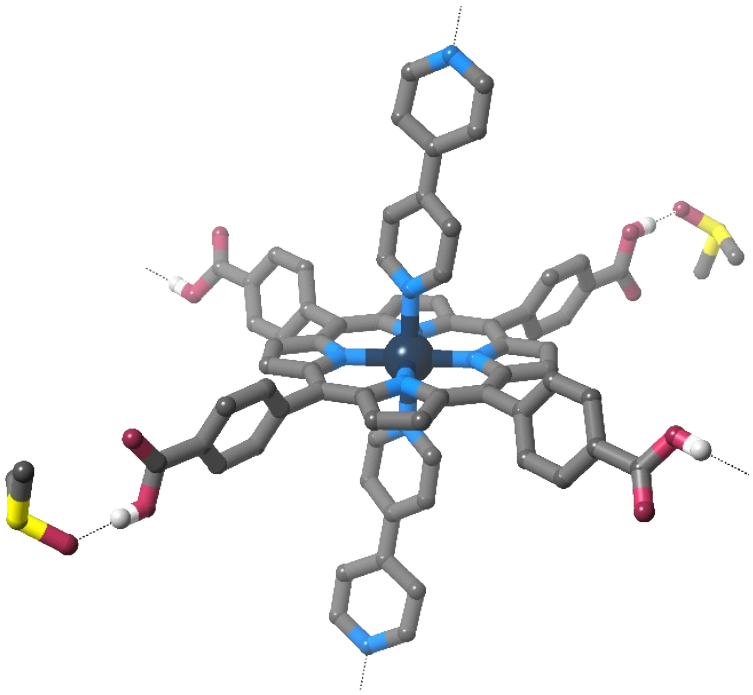

Figure S11. Structure of $[\mathbf{4}^{4H}\cdot(\mathbf{bpy})_2\cdot(DMSO)_2]_n$ grown from DMSO/CH_2Cl_2. The overall structure is almost identical to that grown from DMSO/acetone, see Figure 7 of main manuscript.

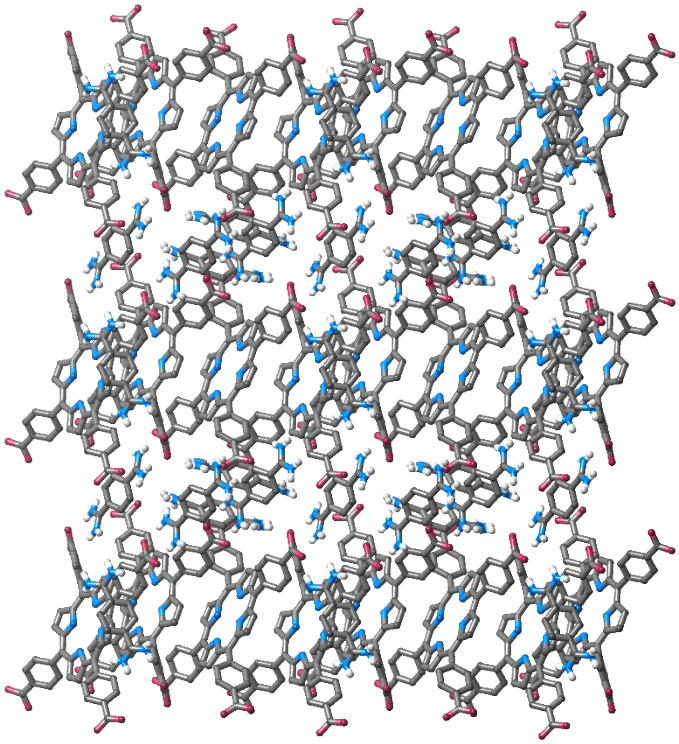

Figure S12. Packing diagram for $\mathbf{2}_2\cdot\mathbf{5}$, viewed down *a*-axis. Most hydrogen atoms omitted for clarity.

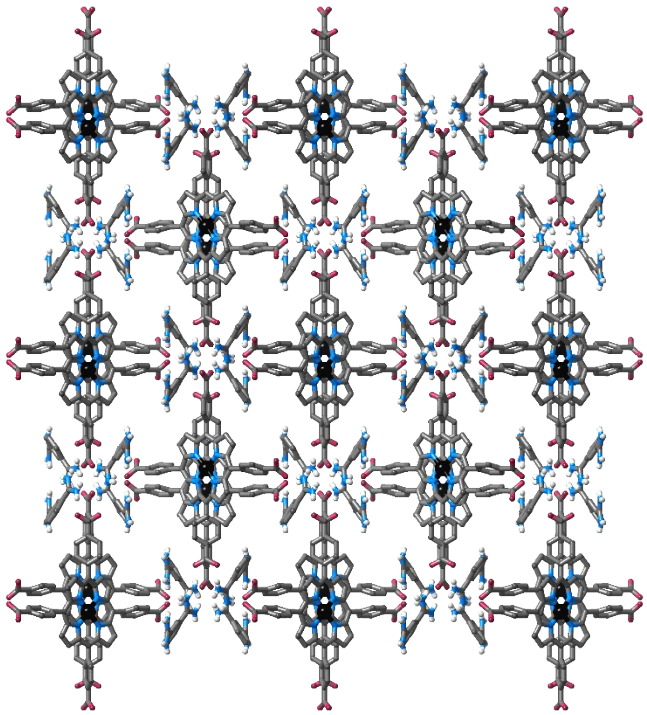

Figure S13. Packing diagram for $\mathbf{3}_2\cdot\mathbf{4}$, viewed down *a*-axis. Water solvent molecules and most hydrogen atoms omitted for clarity.

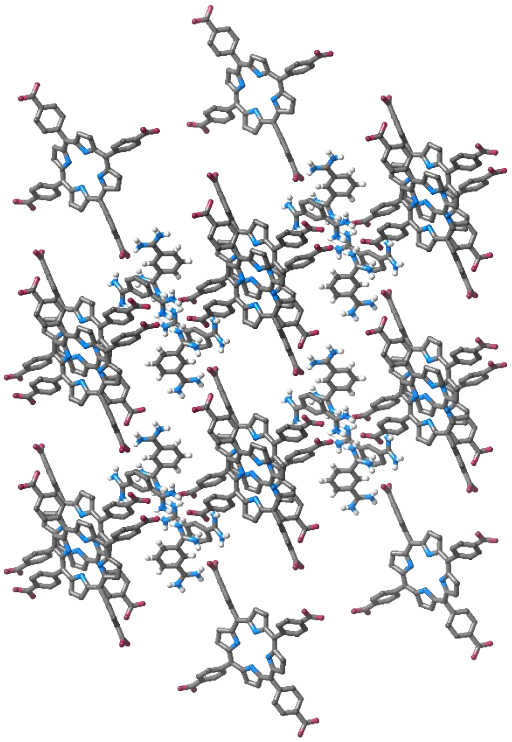

Figure S14. Packing diagram for $\mathbf{3}_2\cdot\mathbf{5}$, viewed down *a*-axis. Pyridine and water solvent molecules and most hydrogen atoms omitted for clarity.

References

[S1] M. Morshedi, M. Thomas, A. Tarzia, C. J. Doonan, N. G. White, *Chem. Sci.* **2017**, *8*, 3019–3025.

[S2] M. Thomas, T. Anglim Lagones, M. Judd, M. Morshedi, M. O'Mara, N. G. White, *Chem. Asian J.* **2017**, *12*, 1587–1597.

[S3] S. Yuan, J.-S. Qin, L. Zou, Y.-P. Chen, X. Wang, Q. Zhang, H.-C. Zhou, *J. Am. Chem. Soc.* **2016**, *138*, 6636–6642.

[S4] H. E. Gottlieb, V. Kotlyar, A. Nudelman, *J. Org. Chem.* **1997**, *62*, 7512–7515.

[S5] S. Venkataramani, U. Jana, M. Dommaschk, F. D. Sönnichsen, F. Tuczek, R. Herges, *Science*, **2011**, *331*, 445–448.

[S6] T. M. McPhillips, S. E. McPhillips, H. J. Chiu, A. E. Cohen, A. M. Deacon, P. J. Ellis, E. Garman, A. Gonzalez, N. K. Sauter, R. P. Phizackerly, S. M. Soltis, P. Kuhn, *J. Synchrotron Radiat.* **2002**, *9*, 401–406.

[S7] W. Kabsch, *J. Appl. Crystallogr.* **1993**, *26*, 796–800.

[S8] G. M. Sheldrick, *Acta Crysallogr.* **2015**, *A71*, 3–8.

[S9] G. M. Sheldrick, *Acta Crysallogr.* **2015**, *C71*, 3–8.

[S10] O. V. Dolomanov, L. J. Bourhis, R. J. Gildea, J. A. K. Howard, H. Puschmann, *J. Appl. Crystallogr.* **2009**, *42*, 339–341.

[S11] J. Cosier, A. M. Glazer, *J. Appl. Crystallogr.* **1986**, *19*, 105–107.

[S12] Agilent Technologies, *CrysAlisPro*, **2011**.

[S13] L. Palatinus, G. Chapuis, *J. Appl. Crystallogr.* **2007**, *40*, 786–790.

[S14] P. W. Betteridge, J. R. Carruthers, R. I. Cooper, K. Prout, D. J. Watkin, *J. Appl. Crystallogr.* **2003**, *36*, 1487.

[S15] R. I. Cooper, A. L Thompson, D. J. Watkin, *J. Appl. Crystallogr*. **2010**, *43*, 1100–1107.

[S16] A.L. Spek, *J. Appl. Crystallogr.* **2003**, *36*, 7–13.

[S17] H. D. Flack, G. Bernardinelli, *J. Appl. Crystallogr.* **2000**, *33*, 1143–1148.

[S18] A. L. Spek, *Acta Crystallogr.* **2015**, *C71*, 9–18.